JOURNAL OF GEOPHYSICAL RESEARCH, VOL. 106, NO. D17, PAGES 20,465–20,481, SEPTEMBER 16, 2001

Changes in the global atmospheric methane budget over the last decades inferred from ^{13}C and D isotopic analysis of Antarctic firn air

Maya Bräunlich,[1] Olivier Aballain,[2] Thomas Marik,[1] Patrick Jöckel,[1] Carl A.M. Brenninkmeijer,[1] Jerome Chappellaz,[2] Jean-Marc Barnola,[2] Robert Mulvaney,[3] and William T. Sturges[4]

Abstract. The atmospheric trend of methane isotopic ratios since the mid-20th century has been reconstructed from Antarctic firn air. High volume air samples were extracted at several depth levels at two sites in East Antarctica. Methane concentration and its $^{13}C/^{12}C$ and D/H ratios were determined by gas chromatography, mass spectrometry, and infrared spectroscopy. A firn air transport model was applied to reconstruct past atmospheric trends in methane and its isotopic composition. By subsequent application of an atmospheric model, changes in methane sources and OH sink compatible with the past atmospheric trends are explored. In step with increasing methane mixing ratios, $\delta^{13}C$ increased by ~1.7‰ over the last 50 years. These changes mainly reflect a shift in relative source strength toward the heavier anthropogenic methane source, such as biomass burning and methane of nonbiological origin. The δD (CH_4) showed a period of decline between the 1950s and 1975, followed by a gradual increase of 0.55‰/yr, also toward the heavier anthropogenic source. Dependent on possible changes in the OH sink, to which δD of methane is very sensitive, the inferred isotopic trends of $\delta^{13}C$ and δD over the last 50 years constrain the relationship between natural and anthropogenic sources over the last century. The observed δD minimum around 1975 suggests that the slowing down in the methane source growth took place during this period.

1. Introduction

The atmospheric abundance of methane has more than doubled over the past 200 years, thus affecting the chemistry of the global atmosphere and also the Earth's radiation balance. Methane is closely coupled to atmospheric OH, the principal atmospheric oxidizing species, and methane is also responsible for nearly 20% of the current anthropogenic greenhouse forcing [*Lelieveld et al.*, 1998]. The cause of the large increase from the pre-industrial 730 nmol/mol to the present 1720 nmol/mol [*Etheridge et al.*, 1998, and references therein] is not known in detail. Increasing anthropogenic methane emissions from the industrial (e.g., fossil fuel sources and landfills) and agricultural sectors (e.g., rice paddies, ruminant animals, and biomass burning) are probably the main factors. In addition, the main sink for methane, i.e., the reaction with OH, may have simultaneously decreased [*Thompson*, 1992, and references therein]. The isotopic composition of atmospheric methane [*Stevens and Rust*, 1982] can be used to better constrain the large uncertainties in present methane budget estimations, as has been shown in several studies [*Fung et al.*, 1991; *Kandilar and McRae*, 1995; *Brown*, 1995; *Andersen*, 1996; *Hein et al.*, 1997; *Levin et al.*, 1999]. Individual source types have typical ^{13}C and D isotopic signatures that reflect different methane production processes [e.g., *Levin et al.*, 1993; *Wahlen*, 1993]. Methane from biogenic (bacterial) origin is highly depleted in both ^{13}C (~-60‰) and D (~ −300‰), whereas methane from nonbiogenic sources is considerably depleted ($\delta^{13}C \approx -40‰$, $\delta D \approx -200‰$). Typical values for methane from fossil fuel combustion are $\delta^{13}C \approx -30‰$ and $\delta D \approx$ -100‰. For methane from incomplete combustion of biomass $\delta^{13}C$ values of $\approx -30‰$ and δD values of $\approx -210‰$ [*Snover et al.*, 2000] are reported. Sink processes also affect the isotopic composition of methane via isotopic fractionation [*Saueressig*, 1999]; e.g., reaction with OH (^{13}C ~ 4‰, D ~ 290‰), with $O(^1D)$ (^{13}C ~ 11‰, D ~ 105‰) and Cl (^{13}C ~ 66‰, D ~ 508‰) in the strato-

[1]Max-Planck Institute for Chemistry, Mainz, Germany.
[2]Laboratoire de Glaciologie et Géophysique de l'Environnement, Grenoble, France.
[3]British Antarctic Survey, Cambridge, England.
[4]School of Environmental Sciences, University of East Anglia, Norwich, England.

Paper number 2001JD900190.
0148-0227/01/2001JD900190$09.00

sphere, and oxidation in soils ($^{13}C \sim 21‰$, $D \sim 66‰$). Consequently, $\delta^{13}C$ and δD reflect changing source and sink contributions to the methane budget.

Historical information about the isotopic ratios of methane in the atmosphere is still limited. *Stevens* [1988] pioneered the investigation of atmospheric $\delta^{13}C$ trends in the Northern and Southern Hemispheres. Since then other attempts have been made for long-term monitoring of this signal at various sites [*Quay et al.*, 1996; *Lowe et al.*, 1999, and references therein], including δD [*Marik*, 1998], providing some information over the last decade. The recent analysis of the Cape Grim air archive and firn air samples collected at Law Dome in Antarctica have extended the history of $\delta^{13}C$ to the last 20 years [*Francey et al.*, 1999]. This study showed an increase of ~0.6‰ in $\delta^{13}C$ since 1978, while the methane mixing ratio increased by ~200 nmol/mol. The authors concluded that global methane sources and sinks probably remained constant since 1982 and that the trend observed in $\delta^{13}C$ reflects the slower equilibration of isotopic signals in the atmosphere compared to mixing ratios. Other historical information on methane isotopic trends is provided by ice core measurements. The only such record to date, suggests an increase in $\delta^{13}C$ of ~2‰ since pre-industrial times [*Craig et al.*, 1988]. The authors interpreted this in terms of a biomass burning source strength in the present-day methane budget, which would amount to ~50 Tg/yr.

In the present study we analyzed air extracted from Antarctic firn (unconsolidated snow), spanning several decades owing to the time required for gas diffusion in this porous medium. The advantage of firn lies in the possibility of extracting much larger amounts of air compared to ice cores, which makes it possible to study with greater accuracy and smaller risk of contamination the decadal to secular history of trace gases of low abundance, including their isotopic composition. An additional rationale for collecting very high sample volumes was to allow measurements of ^{14}CO with an abundance of ~20 molecules per cm^3 (STP) and other ultra rare atmospheric trace gases.

Here we report measurements and modeling of methane mixing ratios including its stable isotopes, ^{13}C and D, from two drilling sites in Antarctica in order to reconstruct their evolution in the atmosphere over the last 50 years. In a second step we interpret these reconstructed trends, with the help of an atmospheric model, in terms of changing ratios of natural to anthropogenic methane sources over time. Because of the high sensitivity of δD levels to changes in OH mixing ratios, this will be done with regard to potential changes in the OH sink.

2. Antarctic Sampling Sites

The first drilling conducted by the British Antarctic Survey took place in Dronning Maud Land (DML) (77° S, 10° W; 2300 m asl) in January 1998. The site has a mean annual temperature of −38 °C and a relatively high snow accumulation rate (60 $kg\,m^{-2}\,yr^{-1}$) compared with the Antarctic plateau. Eighteen firn air samples were taken starting from the surface to the firn-ice transition zone at 73.5 m. Similarly, in January 1999, drilling and firn air sampling was conducted by the British Antarctic Survey and the Laboratory of Glaciology and Geophysics of the Environment (LGGE) at Dome Concordia (DC) (75° 06′ S, 123° 23′ E, 3233 m asl). This is an extremely cold site (−53 °C) with a low accumulation rate (30 $kg\,m^{-2}\,yr^{-1}$) and a deep firn-ice transition zone. At this site, 20 air samples were taken down to the firn-ice transition at 99.5 m.

The sampling of firn air was first documented by *Schwander* [1993]. Here we describe a modified setup for the extraction of large firn air samples of up to 1000 L. Drilling progressed stepwise in intervals of 1 to 5 m. At each level the drill was withdrawn and the hole sealed close to the bottom with a 5 m (DML) or 3 m (DC) long inflatable rubber bladder. Two continuous, 105 m long, 3/8 inch perfluor alkoxy alkane (PFA) tubes passed through the bladder, connecting the pumping system at the surface to the bottom of the hole. Through one of those tubes, ending just below the aluminum end cup of the bladder, air was drawn continuously at high flow rate (25 $L\,min^{-1}$) to waste. The sample air itself was drawn at lower flow rate (15 $L\,min^{-1}$) via the other tube, which ended ~10 cm lower. Both inlets were separated by a set of metal baffles. The function of these baffles (originally devised by M. Bender, Princeton University) is to prevent any possible contamination from the bladder material or leakage pass the seal from reaching the sample inlet at the very bottom of the hole.

The quality of the sampling was continuously monitored with an infrared CO_2 analyzer (Li-Cor) attached to the sample air stream of pumped gas and calibrated with a standard gas. Stable CO_2 levels (less than 0.2 μmol/mol variation) were usually encountered after ~10 min flushing following inflation of the bladder. Purging and filling the different types of sample flasks at each depth level usually required ~2 hours and 1200 L of firn air. The maximum difference in CO_2 mixing ratio observed between the start and the end of sampling was 1 μmol/mol at DC.

A high purity air extraction system was deployed consisting of a two-stage metal bellows pump (Parker) for filling small cylinders, i.e., for LGGE 0.5 L CSIRO glass flasks pressurized at 25 psi. Subsequently, the air emerging from the metal bellow pump was fed into a three-stage, oil-free, modified RIX SA3 piston compressor [*Mak and Brenninkmeijer*, 1994], which allowed the high volume air samples for the Max Planck Institute (MPI) to be compressed to ~120 bars in 5 or 10 L aluminum cylinders (Scott Marrin).

3. Measurements

In this paper we report the first δD measurements of methane from firn air, using the Methane Isotopomer Spectrometer (MISOS) developed by *Bergamaschi*

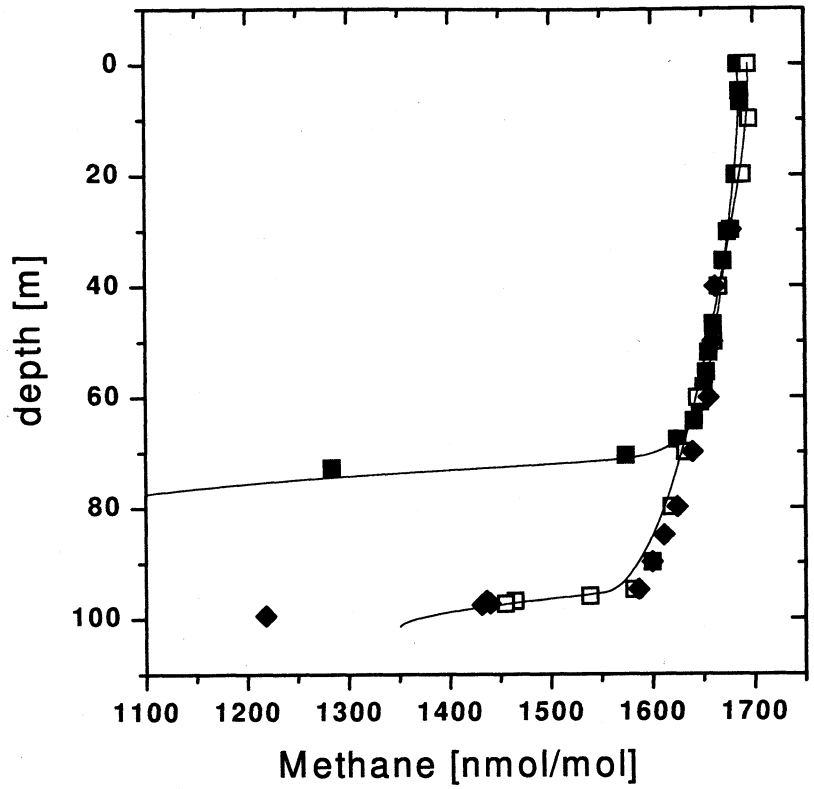

Figure 1. Methane mixing ratios measured by MPI (squares) and LGGE (diamonds) against firn depth at Dronning Maud Land (solid squares) and Dome Concordia (open squares and solid diamonds), compared to firn air diffusion model simulations (continuous lines) for the two sites.

[1994]. For ^{13}C the analysis were carried out in two laboratories, MPI and LGGE, using mass spectrometry. The LGGE ^{13}C measurements are the first reported on atmospheric samples using a continuous-flow technique on very small aliquots.

The high volume samples allowed a wide range of trace gases to be analyzed, which will be reported elsewhere. At MPI, gas chromatography (GC) analysis for CO, CH_4, CO_2, and SF_6 was performed. Further, mass spectrometry was applied for ^{13}C and ^{18}O isotope analysis of CO_2 and CO [*Brenninkmeijer,* 1993]. Analysis of the ^{14}C content of CO, CH_4, and CO_2 were done by accelerator mass spectroscopy.

At LGGE, aliquots of firn air were first used for the determination of CH_4 and CO_2 by GC. Then, $^{13}C/^{12}C$ of CH_4 was measured with a Finigan GC-Combustion interface coupled to a Finnigan MAT 252 isotope-ratio mass spectometer.

3.1. Methane Mixing Ratios

Measurements of methane mixing ratios were made using a GC (HP 6890 at MPI, Varian 3300 at LGGE), equipped with a flame ionization detector. Working reference gases were calibrated for methane against two calibration gases from the National Oceanic and Atmospheric Administration Climate Monitoring and Diagnostics Laboratory (NOAA/CMDL) at MPI, and one calibration gas checked against the NOAA/CMDL scale at LGGE. The overall precision for the firn air samples is estimated to be ±2 nmol/mol for the MPI results and ±4 nmol/mol for those of LGGE.

The data for DML and DC showed the expected decrease in methane with depth (Figure 1). At DML (January 1998) the mixing ratios ranged from the atmospheric level of 1684 ±2 nmol/mol at the surface to 1284 ±2 nmol/mol at the firn-ice transition at 73.5 m. Mixing ratios at DC (January 1999) were 1694±2 nmol/mol at the surface and went down to 1218±10 nmol/mol near the firn-ice transition at 99.5 m. Thus a change in concentration of more than 400 nmol/mol has been observed, reflecting the underlying increase of methane concentration over ~50 years. The two ambient air measurements from January 1998 and 1999 indicate an atmospheric increase of +0.6 %/yr for 1998.

The two methane series of MPI and LGGE at DC agreed well within the uncertainty of the measurements. One notable exception concerns the common sample depth near 97 m, where the MPI results were significantly higher than those of LGGE. The difference was also observed for $\delta^{13}C$ (CH_4) and for CO_2. The most plausible explanation lies in the sequence of sampling, and in the difficulty of recovering firn air in the low open porosity close-off region. The LGGE flasks were the first to be filled after inflating the bladder and, due

to the large amount of air to be sampled, the MPI flasks followed. At this specific depth level, the prolonged pumping may have created a route toward shallower levels in the firn thus filling of MPI flasks with younger air. Therefore only the LGGE results are considered at the DC depth of 97 m in the following discussion and interpretation.

3.2. Stable Isotopes of Methane

The $^{13}C/^{12}C$ and $^{12}CH_3D/^{12}CH_4$ ratios are reported in the usual δ notation, i.e.,

$$\delta^{13}C = \left(\frac{R_{sample}}{R_{std}} - 1\right) \times 1000 \quad ‰, \qquad (1)$$

where R_{sample} and R_{std} denote the $^{13}C/^{12}C$ or D/H ratio, of sample and standard gas, respectively. The ^{13}C analyses were performed at LGGE on a Finnigan MAT-252 mass spectrometer, coupled to a Finnigan GC/combustion interface in continuous flow mode (CF-IRMS). A custom preconcentration unit was used to isolate methane from the major air constituents. This unit included a sample loop of 150 ml, a Haysep D column (20 cm length, 1/8 inch ID) held at $-130\,°C$ with a pentane-ice slush, and a 3 m capillary focussing trap also held at $-130\,°C$, and identical to the main separation column (GS-Q, 30 m length, 0.32 mm ID). After preconcentration, methane was separated from the residual trace gases on the capillary column, combusted to CO_2 and injected with helium into the mass spectrometer for measurement of masses 44, 45, and 46. Isotopic calibration was performed against a pure CO_2 working standard with a $^{13}C/^{12}C$ ratio of -45.98 ± 0.02‰ versus PDB, close to the carbon isotopic ratio of methane in the atmosphere. This value was determined by intercalibration with the MPI standard and with other laboratories measuring methane isotopes. Simultaneously, with the firn air measurements, the external accuracy of the CF-IRMS was determined by regularly analyzing a tank of atmospheric air sampled at Baring Head, New Zealand, on May 27, 1997, by D. Lowe (National Institute of Water and Atmospheric Research, NIWA), with a $\delta^{13}C$ of -47.16 ± 0.05‰ versus PDB. The firn air samples were each measured at least 4 times, using a sample size of only 80 mL STP. The mean reproducibility on replicate firn air samples and the NIWA standard was ±0.05‰.

At MPI mass spectrometry (IRMS, Finnigan MAT 252) was used off-line after combustion of 1/3 of the methane aliquot to CO_2. A complete description of the experimental procedure at MPI is given by *Bergamaschi et al.* [2000]. The CO_2 was measured against a working standard calibrated against NBS-19 and a $\delta^{13}C$ value of -42.465‰ (V-PDB) was derived. For the international isotope standard NZCH [*Brenninkmeijer*, 1990] our measurements gave a value of -47.13‰, close to

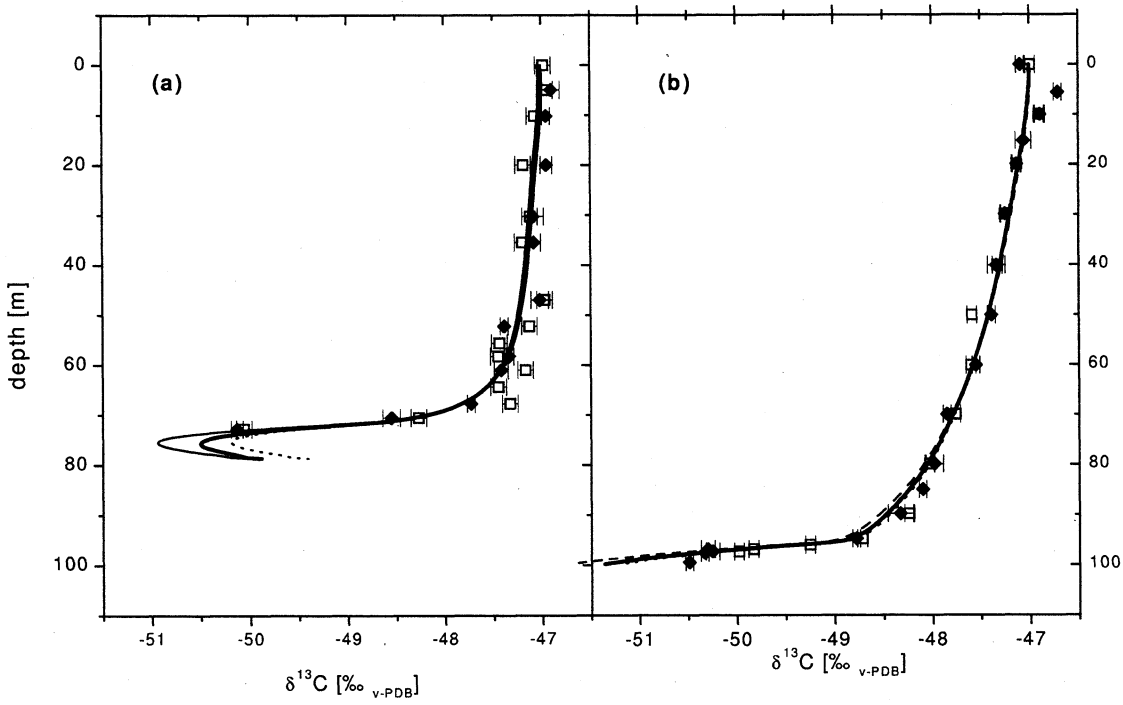

Figure 2. The $\delta^{13}C$ value of methane in firn air at (a) Dronning Maud Land and (b) Dome Concordia, measured by MPI (open symbols) and LGGE (solid symbols). Error bars are 1σ analytical precision and 1σ standard deviation on replicate measurements for MPI and LGGE, respectively. Lines running through the data are firn model results for the best atmospheric $\delta^{13}C$ scenarios (as a function of time in Figure 5) for Dronning Maud Land (dashed line), Dome Concordia (dotted line), and the combination of both sites (solid line).

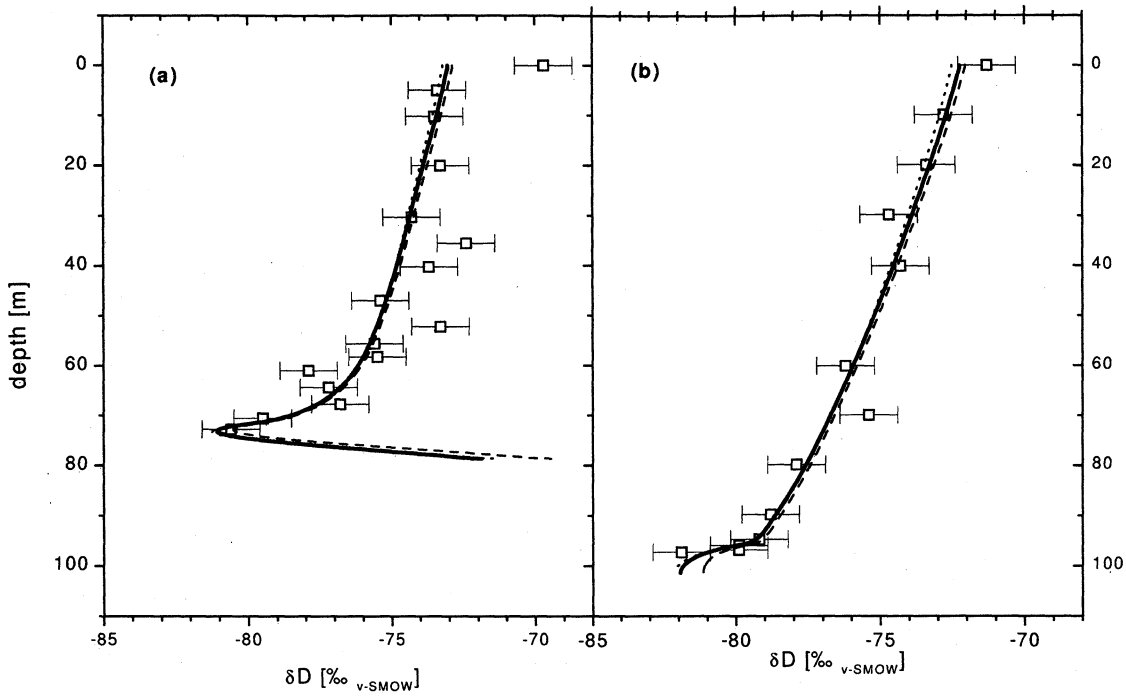

Figure 3. The δD of methane in firn air at (a) Dronning Maud Land and (b) Dome Concordia. Error bars are 1σ analytical precision. Lines running through the data are firn model results for the best atmospheric δD scenarios (as a function of time in Figure 6) for Dronning Maud Land (dashed line), Dome Concordia (dotted line), and the combination of both sites(solid line).

the $\delta^{13}C$ value of $-47.12‰$ based on a laboratory intercomparison [*Röckmann,* 1998]. The low abundance of methane in the older firn air samples necessitated the recovery of methane after the MISOS D/H measurements for subsequent combustion, instead of splitting samples as is usually done [*Bergamaschi et al.,* 2000]. The resulting measurement error in $\delta^{13}C$ was estimated to be $\pm 0.08‰$ for the DML data. The recovery was improved in 1999 and the measurement error thus reduced to $\pm 0.04‰$ for the DC data. Regarding the LGGE measurements of the DML samples (Figure 2a), made on residual air in the MPI flasks, a $+0.25‰$ correction was applied, which takes into account a mass spectrometer nonlinearity effect caused by peak intensity differences between standard and sample on this set of measurements.

The $\delta^{13}C$ values for DML and DC are shown in Figures 2a and 2b, respectively. At the surface, $\delta^{13}C$ was $-47.0‰$ in January 1998 (DML) and January 1999 (DC). With increasing depth the firn air methane was progressively depleted in ^{13}C and reached $-50‰$ at the firn-ice transition. The $\delta^{13}C$ measurements of both isotope laboratories are plotted together and a good agreement of $\sim 0.02‰$ is observed between the LGGE and MPI profiles. Only near the firn-ice transition of DC (Figure 2b) did the LGGE measurements become slightly lighter relative to those of MPI, most probably due to the sampling artifact discussed later. For DML (Figure 2a) the LGGE data set are significantly less scattered. Between 50 and 70 m the MPI data vary by a factor of 2 more than the estimated measurement error of $\pm 0.08‰$. The contamination effects due to the recovery of the methane from the MISOS system as discussed above might have been more important than expected. Both laboratories measured a significant variation of nearly $0.3‰$ in the top 10 m in the DC record (Figure 2b), most probably reflecting seasonal thermal fractionation of gas isotopes in cold firn compared to the relatively warm surface of the austral summer [*Severinghaus and Brook,* 1999]. This phenomenon impacts the firn composition only over the upper 10-15 m and has no effect deeper down, provided that there was no abrupt climate change at the surface over the time period covered by the firn air samples.

The total $\delta^{13}C$ range measured of nearly $3‰$ from top to bottom of the two profiles is very large compared to direct atmospheric measurements. For example, the seasonal amplitude observed at a remote southern hemisphere station, Baring Head (41° S, 175° E), is around $0.4‰$; the observed trend is smaller than $0.05‰$/yr [*Lowe et al.,* 1994].

Measurements of δD (CH_4) on the MISOS system, which gives CH_3D/CH_4 ratios, are expressed relative to the δD (H_2O) standard V-SMOW. The reference gas has a δ value of $-84.5‰$ V-SMOW [*Bergamaschi et al.,* 2000]. There are no international standards for δD in methane to date, but our scale is the same as used in previous source and sink studies (see introduction). The

δD measurement error including sample preparation is estimated to be $\pm 1‰$.

The δD measurements are shown for DML and DC in Figures 3a and 3b, respectively. The values for the ambient air sample at DML in January 1998 were $-70‰$ and as light as $-80‰$ at the firn-ice transition at 73.5 m. For DC they were $-72‰$ in January 1999 and reached $-82‰$ at 97.5 m. The ambient air at DML and DC was 2 to 3‰ enriched compared to the shallowest firn air.

Thermal fractionation of the order of 0.3‰ as encountered in the $\delta^{13}C$ firn profile is unlikely to be detected for δD measurements with the present resolution of $\pm 1‰$. In addition, it would be overwhelmed by the seasonality of the atmospheric signal for δD propagating in the shallow firn. As we will show later, the firn integrates seasonal variations after the first few meters. This means that the annual average should be $\sim -73.4‰$ in 1998 and $\sim -73.0‰$ in 1999. The strong kinetic isotope fractionation of nearly 300‰ in the CH_4 + OH reaction drives a strong seasonal δD cycle, which reaches its maximum in May, beyond the summer maximum in OH. For January, ambient air measurements for δD are expected to be close to the annual mean value and not 2 to 3‰ enriched as observed. The measured difference between the ambient air samples and the first firn air samples is not expected and has no explanation at the moment. The fact that coherent atmospheric scenarios from DML and DC can be drawn from the firn profiles (next Section) suggests that there was no significant artifact in the firn (supposedly temperature, chemical composition, or density related) disturbing the δD signal, and that at least the relative trend in δD is robust.

As for the $\delta^{13}C$ variation, the observed δD range of $\sim$10‰ from top to bottom is high compared to present atmospheric variations. For instance, a seasonal cycle of 4‰ in East Antarctica has been deduced for Neumayer Station (70° S, 8° W), after calculating monthly mean values over a 6 year period [*Marik,* 1998]. In the following section, we will use a model of gas diffusion in firn to reconstruct the past atmospheric isotopic signal from the firn air data.

4. Firn Air Model

Firn is a medium permeable to gases, with increasing density and correspondingly decreased diffusivity from the surface (typical density of 300 $kg\,m^{-3}$) to the firn-ice transition (typical density 850 $kg\,m^{-3}$). Variations in atmospheric trace gas mixing ratio occurring at the surface continuously propagate downwards by molecular diffusion and under the effect of gravitation, and the atmospheric variations are attenuated by this diffusive mixing. In general, light gases such as methane diffuse faster downwards whereas gravitational settling favors the accumulation of the heavier gases in the deepest part of the firn. Owing to these two main processes, mixing ratios as well as isotopic ratios are modified.

For reconstructing an atmospheric history of the methane isotopic ratios from the convoluted firn air signals, we apply the firn air transport model developed by *Rommelaere et al.* [1997]. The main assumptions in this model are that climatic (temperature and accumulation rate) and firn structural variables remain constant in time, and thus also the firn diffusivity profile and depth of the firn-ice transition.

The assumption of a constant temperature is not valid for the top 10-15 m, where seasonal variations propagate and, as a result, thermal fractionation of gases occurs. The impact of these effects is obvious from the $\delta^{13}C$ signal of DC (Figure 2b) but has also been detected for $\delta^{15}N(N_2)$ and $\delta^{18}O(O_2)$ for the DML and DC samples (R. Neubert and M. Leuenberger, personal communication, 1999). To circumvent this problem, we only consider the measurements below 10 m. This does not introduce systematic errors as long as seasonal variations of a trace gas are averaged during the downward diffusion and not reinforced by the seasonal variations in thermal diffusion [*Trudinger et al.,* 1997; *Severinghaus and Brook,* 1999]. The factors that determine gas transport and mixing in the firn are molecular weight, molecular diffusion coefficient, pressure, temperature, and the porosity and tortuosity profiles of the firn matrix. The porosity profile is closely linked to the density profile of the firn. The effective diffusivity of a specific gas in the firn will depend on the porosity profile as well and on the molecular diffusivity of the pure gas in air. The profile of effective diffusivity is the main unknown in the model. We infer it, as proposed by *Fabre et al.* [2000], by calibration with a trace gas of well-known atmospheric evolution. Here we use the CO_2 history, based on atmospheric CO_2 monitoring since 1958 [*Keeling and Whorf,* 2000] and ice core measurements [*Etheridge et al.,* 1996]. Once the effective diffusivity profile has been calibrated for CO_2 the mixing ratio of any trace gas in the atmosphere can be computed by inversion techniques from its firn profile, its molecular diffusivity and its mass as described by *Rommelaere et al.* [1997]. This is true for all gases which do not react with the surrounding snow or ice.

In order to validate the diffusivity profiles for DML and DC, calibrated with CO_2 measurements, we apply the firn model to known atmospheric methane records. A fit through atmospheric measurements from Palmer Station (NOAA/CMDL), starting in 1978, and on ice core measurements [*Etheridge et al.,* 1992] is taken as input of the firn model. The model-generated DML and DC methane profiles are shown in Figure 1 together with our measurements. The agreement between the data and the model reconstruction based on the CO_2 calibration is excellent for DML. For DC a difference of $\sim$10 nmol/mol is observed around 90 m, representing less than the equivalence of one year of atmospheric

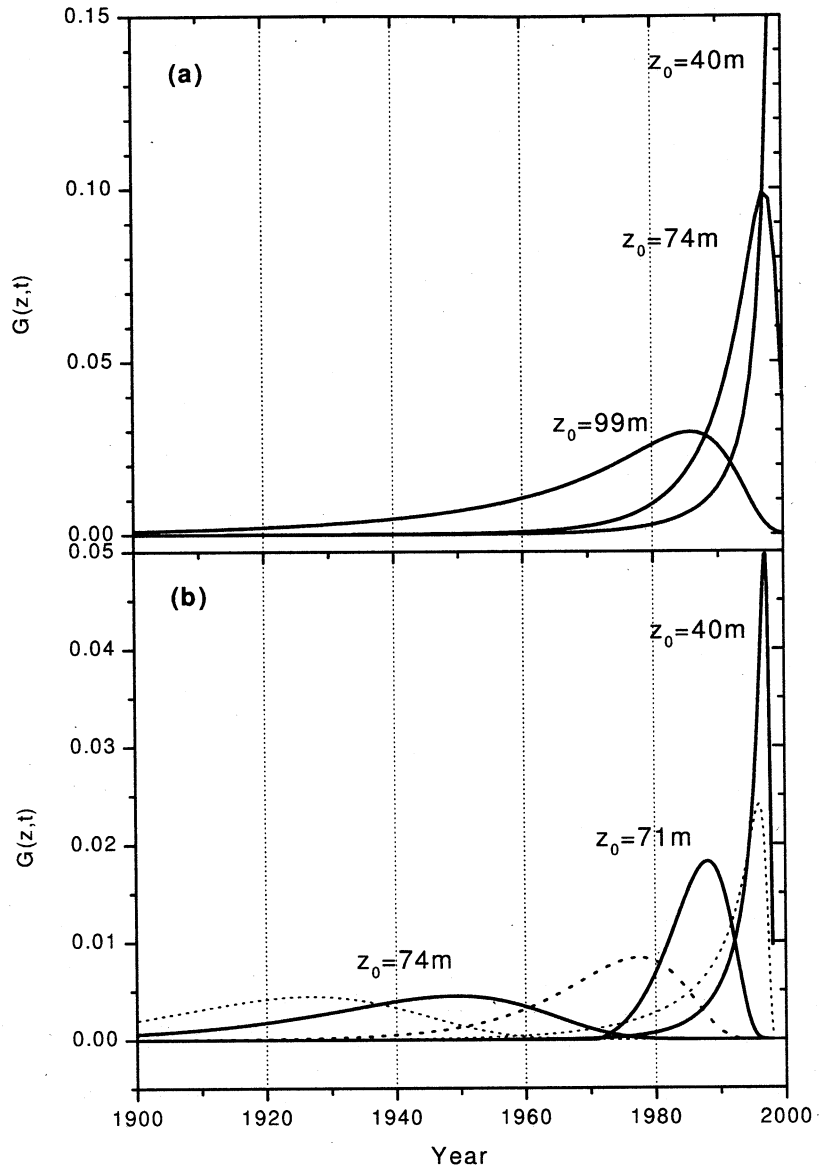

Figure 4. (a) Firn air age distribution for methane at depth z_0 for Dronning Maud Land, plotted as the transfer function $G(z,t)$ (model output) for different values of z_0. (b) Firn air age distribution for methane at Dome Concordia.

evolution during industrial times. The mixing ratio of 1240 nmol/mol from the deepest firn air sample in DC could not be reproduced by the firn diffusion model, because density data suggest that this level is below the firn-ice transition, whereas the model requires open pores for the reconstruction of firn air mixing ratios. Because of the limited amount of air which could be pumped from this depth, no large air sample was taken. We refer to *Fabre* [2000] for a detailed discussion of the DC diffusivity profile, compared to other sites.

The firn air model allows the calculation of the age distribution of any trace gas with depth. This is shown in Figure 4 for methane at DML and DC. At both sites, contemporary air was still contributing significantly to the firn air of the top 40 m, while the average gas age rapidly increased toward the firn-ice transition. The age distribution can be very different from site to site. In general, there is a trade off between high, "cold" sites with low accumulation rates and lower, "warmer" sites, which tend to have higher accumulation rates. Cold sites as DC will have a deeper firn-ice transition zone and thus covering a broader timescale than warmer sites like QML with a more swallow firn-ice transition zone. On the other hand, the lower accumulation rates in DC will result in a lower time resolution, i.e., in age distributions which are larger than in QML.

5. Reconstruction of Past Changes in the Isotopic Composition of Methane

Although routinely used for mixing ratios, the implementation of the inverse technique to isotope ratios

Table 1. Range of Free Parameters and Best Scenarios Used in Monte Carlo Runs of the Firn Air Diffusion Model to Get the Best Agreement Between Modeled and Measured Firn Profiles

Monte Carlo Parameters	Parameter Space	Best Scenario	Envelope
$\delta^{13}C$ (1950), ‰	−52.0 - −46.0	−48.75	±0.5
$\delta^{13}C$ (1950), ‰/yr	±1	0.0	±0.1
$\delta^{13}C$ (1999), ‰	−47.1 - −46.9	−47.0	±0.05
$\delta^{13}C$ (1999), ‰/yr	±0.5	0.03	±0.02
δD (1950), ‰	−85.0 - −50	−73.8	±3.9
δD (1950), ‰/yr	±2	−0.58	±0.6
δD (1999), ‰	−74.0 - −70.0	−72.2	±0.3
δD (1999), ‰/yr	±2	+0.82	±0.16

in the firn air model is not yet operational, owing to the nonlinearity of the forward model in the case of isotopes. We have instead used a Monte Carlo approach where scenarios of temporal trends in the isotopic composition of atmospheric methane were tested against the firn air profiles with the firn air model run in forward mode.

Since the firn air model is linear with regard to mixing ratios, each isotopomer ($^{12}CH_4$, $^{13}CH_4$, and CH_3D) derived from (1) could be calculated separately by the firn air model. Subsequently, the model results were recombined to give $^{13}CH_4/^{12}CH_4$ and $CH_3D/^{12}CH_4$ ratios and the δ values calculated, using equation (1), and compared with the measured δ values. The diffusion coefficient for methane and its isotopomers in air was calculated after *Bzowski et al.* [1990]. Experimental estimates of the ratio of diffusion coefficients for $^{13}CH_4$ and $^{12}CH_4$, made on dry porous bentonite with a binary mixture of nitrogen and methane, show a remarkable agreement with the theoretical value [*Pernaton et al.*, 1996].

5.1. Monte Carlo Modeling

The atmospheric evolution (the firn air model input) was parameterized as a third-order polynomial defined in the time interval 1950 to 1998 (DML) and 1999 (DC). Sensitivity studies showed that atmospheric methane changes prior to 1950 hardly influenced the reconstructed firn air records at DML and DC.

We also tested linear and quadratic scenarios, which restricted the reconstructed results considerably, whereas the results from polynomials of higher order did not add new information within the experimental uncertainty. The third-order polynomial scenarios were set up with four free parameters: the δ value and yearly rate of change in 1950 and in 1999. Ten thousand depth profiles (the firn model output) for $\delta^{13}C$ and δD were calculated with the firn air model for DML and for DC, varying the polynomial coefficients, i.e., the four free parameters, at random within the limits given in Table 1. In a first step, the parameter space was considerably larger in order to test that no other solution exists. For the final reconstruction the parameter range was narrowed down iteratively to the values given in Table 1.

The resulting firn model depth profile, which best reproduced the measurements, defines the most likely reconstructed atmospheric methane isotopic evolution of the past 50 years. In order to obtain this best scenario we define the error function

$$E = \sum_{i=1}^{n} \sqrt{[m(d_i) - \sigma(d_i)]^2} \times \frac{\Delta\sigma(d_i)}{\sum \Delta\sigma(d_i)}, \qquad (2)$$

where $\sigma(d_i)$ are the observations and $m(d_i)$ the model results at depth d. The measurement error $\Delta\sigma(d_i)$ is introduced in order to give different weights to measurements done at LGGE and MPI, and for DML and DC. For $\delta^{13}C$ the measurement errors varied depending on the isotope laboratories and the year of analysis (MPI(1998,DML)=±0.08‰, MPI(1999,DC)=±0.04‰, LGGE(DML,DC)=± 0.05‰). The δD measurements had a reproducibility of ±1‰ for both sites and were only measured at MPI. The ambient air δD values at the surface were not used in the Monte Carlo runs because they are clearly different from the annual mean.

Because there are no known methane sources in the remote high-latitude Southern Hemisphere and the tropospheric air is well mixed, the profiles from DML and DC should represent an identical history. We therefore combined the two sites and performed a third Monte Carlo run (again with 10,000 parameter sets) using identical free parameters for both locations, and tested against both profiles.

5.2. Positive $\delta^{13}C$ Trend Over the Last 50 Years

The reconstructed atmospheric evolution of $\delta^{13}C$ is shown in Figure 5 for the three Monte Carlo runs. The main common feature of the different scenarios is the positive trend in the $\delta^{13}C$ signal over the last 50 years. Among the large range of parameters considered (Table 1), the best defined scenario for each of the three Monte Carlo runs, all lie within a much narrower range. We choose for the best scenario for the combination of DML and DC an error envelope defined by scenarios for which

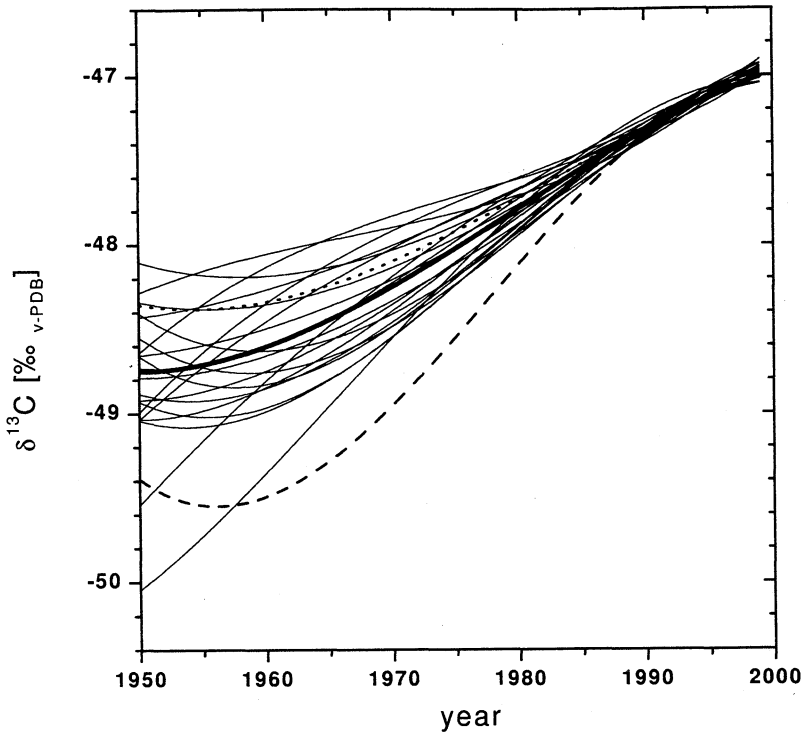

Figure 5. Atmospheric scenarios of $\delta^{13}C$ evolution for the last 50 years, reproducing the firn air profiles in Figure 2 of Dronning Maud Land (dashed line) and Dome Concordia (dotted line), based on Monte Carlo runs of a firn air diffusion model. The best scenario (solid line) reproduces both firn air profiles. The thin solid lines define an error envelopes around the best scenario (see Text). In addition, $\delta^{13}C$ values from the Cape Grim Air Archive (solid symbols) and other firn measurements (open symbols) [*Francey et al.*, 1999] are shown.

the corresponding modeled depth profiles were within a 0.3‰ range of each measurement and for which the Monte Carlo error (equation (2)) was within 5% of the best scenario. In Table 1 the best scenario is given together with its error envelope and it is also plotted in Figure 5. Here we plot only 20 of the above described scenarios defining the outer limits of the error envelope, while the structure of each scenario can still be seen. Close to the best scenario we can find scenarios which compensate higher values in the beginning with later lower values and vice a versa. This is a typical phenomenon for the reconstructed scenarios and is due to the age distribution discussed earlier. The calculated firn profiles corresponding to the best scenarios for DC and DML are compared with the measurements in Figures 2a and 2b.

For the annual trends and for the absolute $\delta^{13}C$ values the Monte Carlo approach has constrained the initial range in the parameter space by at least a factor of 2. The best scenarios generated separately for DML and DC have a very consistent trend for $\delta^{13}C$ of $+0.04\pm0.01$‰/yr over the last 15 years but differ by nearly 1‰ in 1950. The best scenario for DC starts around -48.3 ± 0.5‰ in 1950 and ends after a positive trend over the last 50 years around -47.0 ± 0.05‰ in 1999, whereas the best scenario for DML starts around -49.4 ± 0.7‰ in 1950 but is in very good agreement with the DC scenario from 1985 onwards. For the combined DC and DML Monte Carlo run, Figure 5 shows that the resulting atmospheric scenario is very close to the already extracted best DC scenario. With more samples taken in the deep DC firn compared to DML, together with the improved measurement error at MPI in 1999, the scenarios are all together better defined by the DC measurements. The best DML scenario lies clearly outside the error envelope for the combination of DML and DC, because it reproduces the DC data less precisely at depths around 90 m (see Figure 2b). An interesting feature is the turning point observed in the modeled $\delta^{13}C$ profile near the firn-ice transition zone in DML (75 m). Below 70 m the high firn density leads to an effective diffusion close to zero at DML, even though there are still open pores at this depth. In this layer the firn air age increases dramatically over short distances, and thus the atmospheric trend towards lighter $\delta^{13}C$ values can directly be seen in the firn profile.

In the work of *Etheridge et al.* [1998] a detailed $\delta^{13}C$ record, based on atmospheric methane measurements from the Cape Grim Air Archive and data from Antarctic firn air, was published for the time period 1978 to 1993. While their overall trend is comparable to our reconstructed trend over this period, there

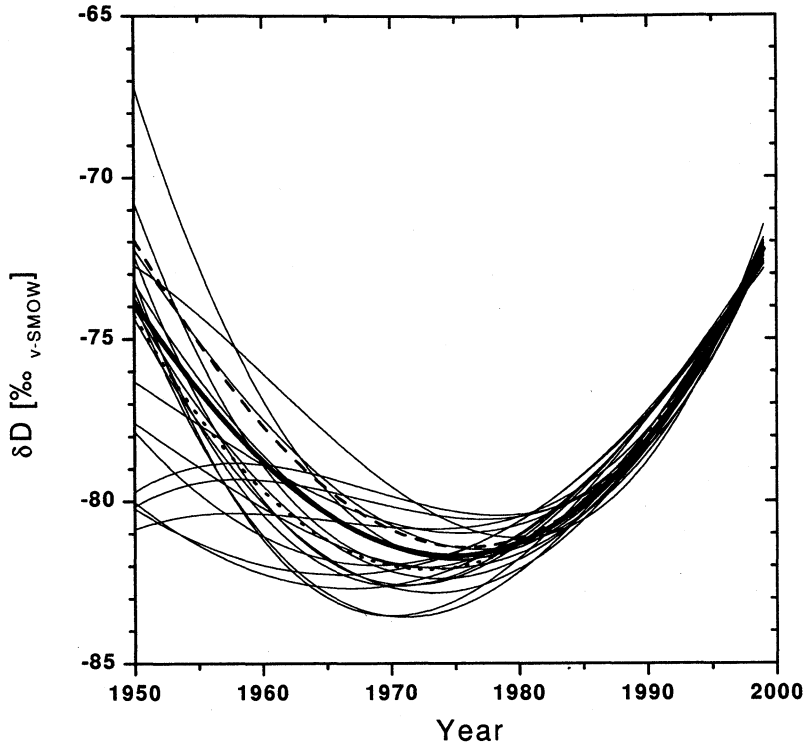

Figure 6. Atmospheric scenarios of δD evolution for the last 50 years, reproducing the firn air profiles in Figure 3 of Dronning Maud Land (dashed line) and Dome Concordia (dotted line), based on Monte Carlo runs of a firn air diffusion model. The best scenario (solid line) reproduces both firn air profiles. The thin solid lines represent error envelopes around the best scenario (see text).

is a significant offset of nearly 0.4‰ between the two data sets. Their δ^{13}C values have subsequently been linked with the NZCH standard [*Francey et al.*, 1999], which now allows a direct comparison with our data (Figure 5). The two data sets now agree within their error specification. From 1978 onward, their observed mean trend over the last 17 years is +0.04‰/yr, which is identical to our mean DC/DML positive δ^{13}C trend of +0.04±0.01‰/yr over the same period. Thus the significantly higher trend reported earlier by *Stevens* [1988], ~+0.14‰/yr from 1978 to 1988, is further questioned.

5.3. Observed Minimum in the δD Record

The past atmospheric evolution of δD in methane is unknown. The δD can be reconstructed with as much confidence as δ^{13}C from firn air samples, even though D/H measurements are difficult and have a measurement uncertainty of ±1‰. Corrections for diffusion and gravitation are basically mass dependent and therefore identical for both stable isotopes. However, the δD variations from top to bottom in the firn air were more than 10‰. This makes the reconstruction of the past atmospheric δD evolution very sensitive to its trend over the last few decades, as will be shown below.

Figure 6 shows the results for δD. The reconstructed scenarios start in 1950 at values between −81‰ and −67‰. They show a clear minimum of between −83‰ and −79‰ in the 1970s and have strikingly similar slopes of 0.55±0.05‰/year over the last two decades. Scenarios with lower starting values tend to have their minima in the early 1980s at higher values. Even with a wide parameter range (Table 1), the best fits through the DML and DC data, separately and combined, gave a very coherent picture. Thus the Monte Carlo technique is able to constrain not only the starting point significantly, but also the present mean atmospheric value of −72.2±0.3‰ and the δD trend over the recent decades. The envelope for the combined scenarios was chosen in a way similarly to that for the δ^{13}C record. The set of scenarios shown corresponds to modeled depth profiles (Figures 3a and 3b) which fitted each measurement within a 3‰ range and for which the associated error was again within 5% of the best scenario. As for δ^{13}C , the modeled profiles for DML showed a change in trend toward enriched isotopic values in the nondiffusive zone near the firn-ice transition. This reflects the atmospheric trend prior to 1975.

Our δD reconstruction is unique and there is little data for comparison. There are unpublished δD data for Neumayer Station (70° S, 8° W) for the period 1989 to 1997 [*Marik*, 1998], which have a much larger experimental uncertainty of ±5‰. Our reconstructed δD trend for 1990 to 1999 of +0.55±0.05‰/year is at the

lower end of the +0.9±0.3‰/year which can be extracted from the Neumayer data. In terms of absolute values, and for discussion of the methane budget (section below), the intercalibration in δD between MPI and other laboratories measuring δD of methane must be addressed. The δD source signatures considered by *Marik* [1998] and used here for the discussion, had to be shifted by an offset of +5.7‰. This factor has been established by comparing parallel methane δD data sets at a remote station [*Bergamaschi et al.*, 2000].

6. Effects of Changing Sources and Sinks of Methane

After reconstructing atmospheric scenarios the next step is to infer changes in the methane sources and sinks that can explain these scenarios. In section 7 the two main features of the atmospheric records, the positive δ^{13}C trend and the observed minimum in the δD record, will first be qualitatively explained. The changes in the isotopic composition of methane in a period of increasing mixing ratios, combined with the delay due to the atmospheric response time [*Tans*, 1997], lead to complex connections, which are analyzed in detail using an atmospheric model.

The uninterrupted positive trend in δ^{13}C (Figure 5) suggests in a first approach a shift from light to heavier sources during recent decades. The present-day δ^{13}C value of about −47‰ [*Quay et al.*, 1999] is not the weighted mean isotopic composition of all sources because of the fractionation accompanying the sink processes (oxidation with OH and Cl in the atmosphere and bacterial oxidation in soils). Estimation of the isotopic composition of methane, averaged over all sources, is based either on the sum of methane sources weighted by their isotopic signatures (bottom-up) or on the present atmospheric isotopic values taking into account relative contribution of the sinks and their kinetic isotopic effect (KIE)(top-down).

Using source distributions from *Lelieveld et al.* [1998] and isotopic source signatures from *Hein et al.* [1996, and references therein], the first approach gives $\delta_S(^{13}C)$ = −55.6±8.6‰ for the mean isotopic composition of the methane sources. The high error reflects the current uncertainties in the methane budget and in the measured isotopic composition of sources.

The second approach gives a δ^{13}C value for the mean source of $\delta_S(^{13}C)$=−52.0±0.8‰. This calculation is based on a sink distribution from *Lelieveld et al.* [1998], and KIEs for the OH sink (88%, with mean OH mixing ratios of 5×10^{-6} molecules/cm^3), oxidation in soils (5%) and for the stratosphere (7%) of 1.0039±0.0004 [*Saueressig*, 1999], 1.021±0.005 [*King et al.*, 1989], and 1.012 [*Brenninkmeijer et al.*, 1995] respectively. This second approach can only be applied to an equilibrium state, as has been shown by *Tans* [1997]. In reality, the rising methane levels in the past have influenced the present atmospheric δ^{13}C values [*Lassey et al.*, 2000]. During nonequilibrium states excess source methane leads to a smaller difference between the atmospheric and the mean source value.

The nonequilibrium effect can be well identified in the reconstructed δD signal. The observed minimum in δD (Figure 6) is partly explained by the large difference between the atmospheric value and the mean isotopic source composition. For an identical sink and source distribution as above and isotopic source signatures from *Marik* [1998, and references therein] bottom-up calculations lead to δ_S(D)=−283±13‰. With an atmospheric global average of -79‰ (*Bergamaschi* [2000] and our firn measurements) and the corresponding KIE factors for the sink processes (KIE^D_{OH} = 1.294 ± 0.018 [*Saueressig*, 1999], $KIE^D_{stratos}$ = 1.19 ± 0.02 [*Irion et al.*, 1996], and KIE^D_{soil} = 1.066 [*Wahlen*, 1993]), top-down calculations give a mean source signature of δ_S(D)=−274 ± 10‰. Again, the high error in the bottom-up calculation is due to current uncertainties, not only in the methane budget but also in the measured isotopic composition of sources. The difference of nearly 18‰ for the mean atmospheric source between the two calculations reflects the far-from-equilibrium state of the current atmosphere. In the calculations of *Marik* [1998], if methane sources remain constant from now on atmospheric δD values would reach their equilibrium state after more than 20 years, and a correction factor of ∼20‰ has to be applied to present-day δD levels. Because the bottom-up calculation considers a steady-state situation, only the top-down calculation is affected by this correction factor, closing the gap of 18‰ between the two approaches for the mean atmospheric δD source.

The nonequilibrium state between sources and sinks leads to the observed decreasing trend for δD between 1950 and the minimum around 1975. High methane growth rates have led to excess source methane which is extremely depleted in δD relative to the atmospheric value. After stabilization and subsequently slowing down of the methane growth rates at the beginning of the 1980s [*Dlugokencky et al.*, 1994], a strong δD increase of +0.55±0.05‰/yr is observed, clearly reflecting the shift toward the heavier atmospheric equilibrium values. The atmospheric model introduced in section 7 will take into account the nonequilibrium state of methane mixing ratios and isotopes in the atmosphere.

7. Changes in Methane Sources and Sinks Using an Atmospheric Model

To quantify the additional constrains for the methane budget gained from our reconstructed trends in δ^{13}C and δD over the last 50 years, we use the atmospheric eight-box model (BOSCAGE-8) from *Marik* [1998]. In this atmospheric model, transport is simulated by the exchange of gases between the lower atmosphere (six

Table 2. Emission rate, Mean $\delta^{13}C$, and δD of Natural and Anthropogenic Sources of Methane Used as Input to the BOSCAGE-8 Atmospheric Model[a]

	Case A OH Constant			Case B OH Decreasing		
	1800	1950	1999	1800	1950	1999
Total source, Tg/yr:	211	354	519	262	375	517
Natural sources	135	135	135	200	200	200
Anthropogenic sources	76	219	384	62	175	317
$\delta^{13}C$ source, ‰	−55.9	−53.1	−52.0	−55.6	−53.4	−52.0
δD source, ‰	−274	−266	−262	−274	−267	−262
source signatures	$\delta^{13}C$	δD		$\delta^{13}C$	δD	
Natural sources	−59.6	−286		−57.9	−281	
Anthropogenic sources	−49.3	−254		−48.3	−250	

[a]Results are given for two cases: A (OH constant), and B (OH decreasing)

latitudinal boxes) and the stratosphere (two boxes north / south). It was designed to simulate long-term atmospheric records of methane mixing ratios and isotope ratios, including their seasonal variations and annual trends.

The modeled tracers are CH_4 (including ^{13}C and D) and SF_6. The model has a time resolution of 2 weeks and SF_6 measurements are used to calibrate the interbox exchange time. The methane source distribution and seasonality is taken from *Hein et al.* [1997], while the source signatures for $\delta^{13}C$ and δD are taken within the range given by present publications (see previous section). The free parameters of the model are the total emission of each source type. Changing sinks will be considered by discussing two different model runs: case A with OH levels kept constant at the present value, and case B with decreasing OH levels in periods of growing methane and CO mixing ratios (see section 8). The sink KIE factors are taken with the values mentioned above. The model outputs have to reproduce (1) the present atmospheric values for $\delta^{13}C$ and δD from Neumayer station (70° S, 8° W) [*Marik,* 1998], (2) methane mixing ratios since 1800 based on Antarctic ice-core records [*Etheridge et al.,* 1998], and (3) present-day atmospheric methane distribution based on the NOAA/CMDL monitoring network.

In order to limit the range of scenarios tested in our simulation of long-term methane and isotopic trends in the high-latitude Southern Hemisphere, we consider two main assumptions about the evolution of methane sources. First, they are divided into two categories, natural and anthropogenic, with the natural source (i.e., wetlands and 10% of the total biomass burning) kept constant over the last 200 years. Second, the increasing anthropogenic source (rice paddies, ruminants, landfills, fossil fuel, and 90% of the total biomass burning) is related to human population growth, as suggested by *Khalil and Rasmussen* [1985]. This assumption will be discussed in more detail together with the model results. In Table 2 the temporal scenarios since pre-industrial times of methane source strengths (natural and anthropogenic) and the mean $\delta^{13}C$ and δD source signatures for the two cases A (OH constant) and B (OH decreasing) are listed. The corresponding Antarctic $\delta^{13}C$ and δD trends calculated with the BOSCAGE-8 model are shown in Figure 7 together with the best estimate from the firn air measurements.

Until 1980 the assumption of an anthropogenic methane source strength proportional to human population is in agreement with changing methane mixing ratios over the past 200 years. After 1980, however, decreasing methane-growth rates [*Dlugokencky et al.,* 1994] make it necessary to decouple the two variables. Therefore we lowered the annual increase of methane sources in 1983 from ~6.3 Tg/yr (+1.3 %/yr) to ~1 Tg/yr (+0.2%) until 1991 and we kept it constant afterward for case A (constant OH). The decreasing OH levels until 1978 in case B result in a slightly lower annual methane source increase before 1983 (+5 Tg/yr).

For $\delta^{13}C$ the comparison of the modeled and firn-based reconstructed evolution of the atmospheric trend over the past 50 years is encouraging (see Figure 7a). Both cases A and B fall within the envelope of scenarios given by the firn model. The positive $\delta^{13}C$ trend corresponds to a calculated increase of the anthropogenic methane source, implicating a positive trend in the mean $\delta^{13}C$ source as listed in Table 2. In contrast, the results for δD scenarios differ significantly from the reconstructed atmospheric δD. For both cases A and B the calculated δD values show a pronounced minimum around 1980, which happens later and is 1 to 3‰ lighter than the firn air-derived δD scenario. As a consequence, the modeled trend over the last 20 years

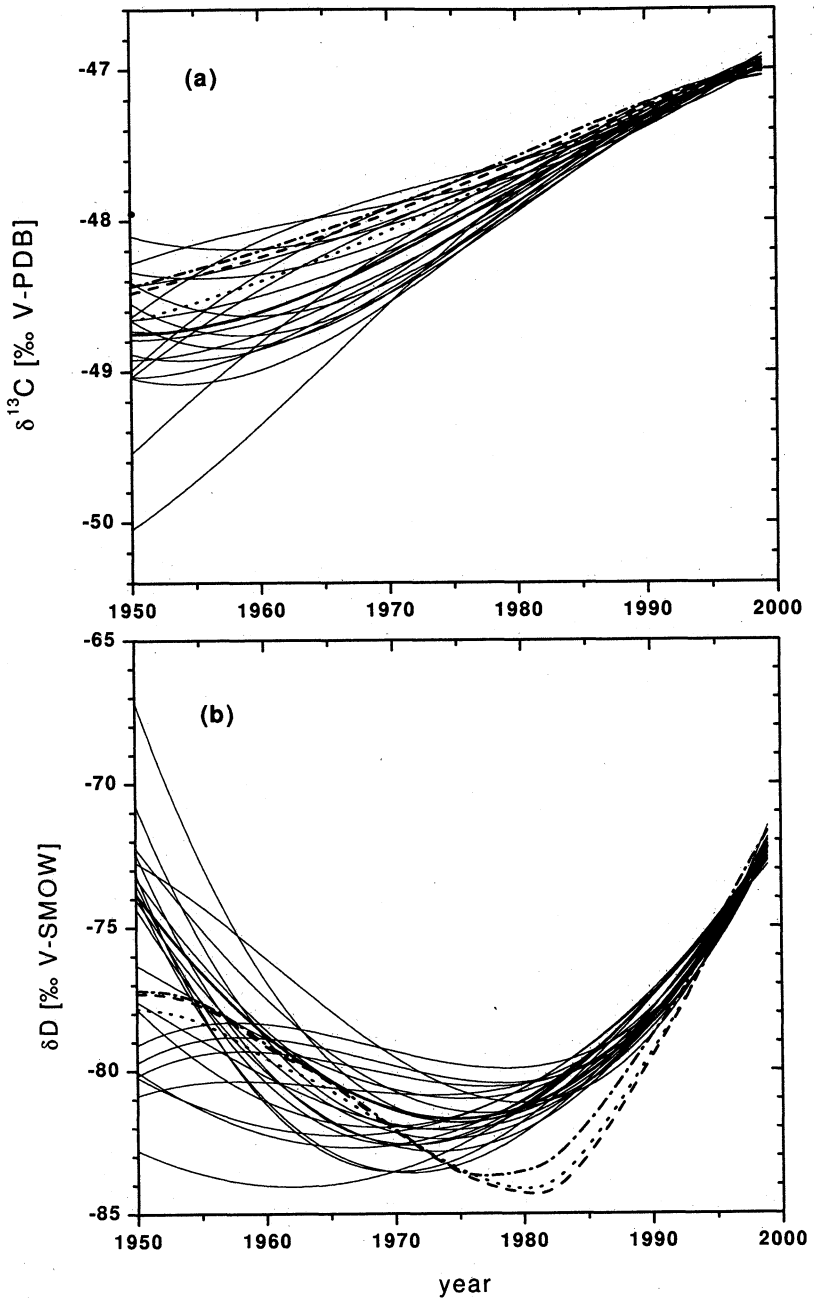

Figure 7. (a) Comparison of three outputs of the atmospheric methane isotope model BOSCAGE-8 with the best scenario (solid line) from reconstruction of the atmospheric $\delta^{13}C$ trend over the last 50 years from Dronning Maud Land and Dome Concordia. The dotted line corresponds to the Case A output assuming constant OH levels over the last 200 years; the dashed line corresponds to case B with OH levels linearly decreasing by 23% from 1885 to 1978. In case C (dash-dotted line) the growth rate of methane sources is optimized to better fit the recent trend in mixing ratios and isotopes. (b) Same for δD.

is more pronounced than the trend reconstructed from the firn profiles (+0.7 instead of 0.55‰/yr). If real, the enhanced gradient over the last two decades would lead to firn profiles depleted by more than 1‰ compared to our δD measurements at DML and DC.

The main parameter, influencing the position of the δD minimum, is the time at which the growth of methane sources started to slow down. The response of atmospheric δD to a decrease in methane growth rates is fast compared to the atmospheric lifetime of methane, because the difference between the sinks and sources decreases and drives the atmosphere towards its equilibrium value. This implies that the δD trend changed from negative to positive values, whereas the positive growth rate of mixing ratios only change in strength from 1 to 0.2 %/yr. This makes mixing ratios less sen-

sitive than the isotopic ratios to any change in the total methane source strength. For the BOSCAGE-8 runs shown in Figures 7a and 7b for $\delta^{13}C$ and δD, respectively, the growth in the methane source was adapted in order to shift the minimum toward 1975 (case C), while trends in mixing ratios and $\delta^{13}C$ still had to be reproduced. The other model parameters were kept unchanged compared to case A. This approach implied for constant OH levels, methane source strengths that changed earlier and less abruptly. The growth rates are stepwise reduced from 1974 onward (before 1974: 6.6 Tg/yr (1.4%); 1974-1981: 5 Tg/yr (1%); 1981-1991: 1.6 Tg/yr; short period of decline from 1991 to 1994: -1.8 Tg/yr) and the methane source strength stays constant at 519 Tg/yr after 1994. This scenario of total methane emissions best reproduces the observed atmospheric mixing ratios, while it still agrees with the firn-based reconstruction of the $\delta^{13}C$ trend (Figure 7a, case C). Nevertheless, for δD even this run (case C, Figure 7b) still lies outside the uncertainty envelope of the firn-based scenario. The calculated δD minimum happens either $\sim$5 years too early or is 1-2‰ too light.

Another parameter influencing the δD minimum, however, is the fractionation factor in the sink process. Sensitivity tests made with the BOSCAGE-8 model in order to shift the minimum by about 1‰ towards heavier values, resulted in a reduction of the mean tropospheric KIE factor from 1.27 to 1.22, by a reduction of the total sink contribution of OH from 88% to 81% towards the soil sink and a reduction of the KIE^{D}_{OH} from 1.294 to 1.250. For the mean δD source this would result in a shift from -262‰ to -255‰, with δD source signatures being at the lower end of their error specification.

The tests described above, although limited, give some indications on the sensitivity of the model output to key parameters. Additional work is needed before the best constrains on the methane budget can be extracted from our data set.

8. Discussion

When assuming that OH levels remained unchanged over the last 200 years, only the increasing anthropogenic source is responsible for growing methane mixing ratios and the positive $\delta^{13}C$ and δD trend towards a heavier equilibrium state in both isotopes. Assuming a constant natural source of 135 Tg/yr, the ratio between natural and anthropogenic sources has decreased since pre-industrial times from $\sim$1.8 to $\sim$0.4. With the mean anthropogenic source being more than 10‰ enriched in $\delta^{13}C$ relative to the mean natural source, the global methane source would have become $\sim$4‰ heavier in $\delta^{13}C$ compared to 1800 and 2‰ heavier since 1950 (Table 2). This potential 2‰ shift is close to our reconstructed trend of 1.7 ± 0.7‰. Thus, even if for all these values the far-from-equilibrium state of the atmosphere is taken into account by the model, the atmospheric $\delta^{13}C$ trend still closely reflects the underlying trend of the mean methane source. The situation is different for δD. Here the difference between mean anthropogenic and natural source is more than 30‰, making the present global source up to 12‰ heavier in δD than compared to pre-industrial values. This time the atmospheric shift in δD values is not comparable to the differences in the mean sources, because of the already mentioned far-from-equilibrium state of the present atmosphere. For the last 50 years the expected shift of 7‰ is less directly seen in the reconstructed scenarios than for $\delta^{13}C$.

When assuming that the OH sink increased by 23% between 1885 and 1978 [*Thompson and Cicerone,* 1986; *Marik,* 1998] the methane increase since pre-industrial times is due to a combination of increasing anthropogenic sources and decreasing sink. In addition, the ratio between natural and anthropogenic sources since pre-industrial times becomes more important (from $\sim$ 3.2 to $\sim$0.6), in order to compensate for the more important sink in pre-industrial times. As we still assume that the natural and anthropogenic sources remained constant and proportional to human population respectively, we need to compensate for the higher isotopic fractionation in the past during elevated OH levels by shifting natural and anthropogenic sources towards heavier values. The δD is far more sensitive to changing OH levels than $\delta^{13}C$, because of the very large fractionation of $\sim$300‰ in this sink process. The mean anthropogenic and natural δD source have thus both to be changed in the range of +5‰ in order to compensate for the increased sink.

Overall, our interpretation of the temporal trends deduced from the firn air profiles suffers from several caveats: (1) the lack of intercalibration laboratories measuring methane isotopes on sources and in the atmosphere (we note that this concerns the absolute δD and $\delta^{13}C$ values, but not the trends derived in this study), (2) the large range of δ values for the sources, (3) the uncertainties in the fractionation factors for the different sinks, (4) the limited number of free parameters (e.g., not including the strength of individual sources, changing natural sources, etc.) tested in the BOSCAGE-8 model so far. All together, this makes it difficult to quantify the evolution of individual methane sources since pre-industrial times from the firn air data alone. Concerning the OH sink, the expected δD trends calculated by BOSCAGE-8 also suffer from the problems listed above. Even if δD is very sensitive to OH changes, we cannot confidently differentiate between the two considered cases A and B with our firn profiles. Still, any future attempt to produce a methane budget on the corresponding time period should be tested against the temporal evolution of the three tracers now available: the mixing ratio and the two stable isotopes.

9. Conclusions

The present data from two Antarctic sites, Dronning Maud Land and Dome Concordia, extend and complete existing records of $\delta^{13}C$ of methane and appear to be

the first ever reported for past δD of methane. A Monte Carlo approach using a firn air model gives the most plausible scenarios of atmospheric trends based on the measured firn profiles. We found very similar reconstructed trends for δ^{13}C and δD for the two Antarctic sites, thus allowing us to combine both firn air profiles and to increase the precision of the reconstruction. We revealed a positive δ^{13}C shift of 1.7±0.7‰ over the last 50 years, with a trend of +0.04±0.01‰/yr over the last 15 years. The latter trend compares very well with previously published δ^{13}C measurements based on the Cape Grim air archive and Law Dome firn air [*Francey et al.*, 1999]. The reconstructed trends of δD revealed a decrease until ~1975 followed by a gradual increase of 0.55±0.05‰/yr over the last 2 decades. The δD minimum reflects the non-equilibrium state between atmospheric methane and its sources and sinks in a period of changing budget. We tested some scenarios of changing methane budget against our temporal reconstruction with the help of an atmospheric eight-box model from *Marik* [1998]. Assuming constant sinks and natural sources over the last 200 years, and an increase in the anthropogenic sources proportional to human population, the model reproduced reasonably well the temporal trend of methane and its stable isotopes until 1975. The minimum in our δD record at that time required a decrease in the growth rate of methane emissions from 6.3 to 5 Tg/yr until 1981, with a further drop afterward to 1.6 Tg/yr until 1991, before methane source strength stabilized from 1994 onward (short period of decline from 1991 to 1994). Over the considered time period we also considered changes in the sink strength. This allowed to change the ratio between the isotopically lighter natural sources and the isotopically heavier anthropogenic sources, which is responsible for the observed shift in the equilibrium value of δ^{13}C and δD toward heavier values. Our present knowledge of the atmospheric methane cycle, including the isotopic information based on atmospheric records, source signatures and kinetic isotope effects of the sinks, permitted us to reproduce our observed positive δ^{13}C trend and the main features of our firn-based δD trend. Nevertheless, the difference in the calculated and observed δD record over the last 2 decades indicates that there may still be some ambiguity in the actual KIE factors, the sink distribution and the applied models. The importance of the methane isotope data from firn air of the last 50 years presented here will increase with higher precision of the source signatures for δD and of the fractionation factors of the sink process. The comparison with firn air measurements going further back in time together with a Northern hemisphere record, defining an interhemispheric gradient, would also put important constraints on the global methane budget. All this will considerably improve our knowledge of changes in the atmospheric source and sink processes of methane that have caused the large increase in methane mixing ratios since pre-industrial times.

Acknowledgments. This work is a contribution to the FIRETRACC/100 Project, under the European Commission Environment and Climate Program (1994-1998) contract ENV4-CT97-0406. It benefited from the field support of the EPICA joint ESF/EC program, of the French polar institute (IFRTP) and of the ENEA Antarctic Project (Italy) at Dome C, and of the British Antarctic Survey at Dronning Maud Land. We thank Adeline Fabre for help in firn air diffusion modelling, Laurent Arnaud for field sampling at Dome C, Dave Lowe and Ingeborg Levin for intercalibration of standards. Additional financial support for the LGGE work was provided by the Programme National de Chimie Atmosphérique (INSU-PNCA) and by the European Program EPICA (contract ENV4-CT95-0074). J.C. expresses his gratitude to John Hayes (Woods Hole Oceanographic Institute, formerly at Indiana University) and to Jean Jouzel (CEA/LSCE) for early advice and help in the development of the continuous-flow technique at LGGE.

References

Andersen, B. L., Modeling isotopic fractionation in systems with multiple sources and sinks with application to atmospheric CH_4, *Global Biogeochem. Cycles, 10*, 191-196, 1996.

Bergamaschi, P., M. Schupp, and G.W. Harris, High-precision direct measurements of $^{13}CH_4/^{12}CH_4$ and $^{12}CH_3D/^{12}CH_4$ ratios in atmospheric methane sources by means of a long-path tunable diode laser absorbtion spectrometer, *App. Opt., 33*, 7704-7716, 1994.

Bergamaschi, P., M. Bräunlich, T. Marik, and C. A. M. Brenninkmeijer, Measurements of CH_4 and its carbon and hydogen isotopes at Izana, Tenerife - Seasonal cycles and synoptic scale variations, *J. Geophys. Res., 105*, 14,531-14,546, 2000.

Brenninkmeijer, C. A. M., A light carbonate standard for ^{13}C analysis of atmospheric methane, *Rep. INS-R-913*, Inst. Nucl. Sci., Lower Hutt, New Zealand, 1990.

Brenninkmeijer, C. A. M., Measurement of the abundance of ^{14}CO in the atmosphere and the $^{13}C/^{12}C$ and $^{18}O/^{16}O$ ratio of atmospheric CO, with application in New-Zealand and Antarctica, *J. Geophys. Res., 98*, 10,595-10,614, 1993.

Brenninkmeijer, C. A. M., D. C. Lowe, M. R. Manning, R. J. Sparks, and P. F. J. van Velthoven, The ^{13}C, ^{14}C, and ^{18}O isotopic composition of CO, CH_4 and CO_2 in the higher southern latitudes lower stratosphere, *J. Geophys. Res., 100*, 26,163-26,172, 1995.

Brown, M., The singular value decompostion method applied to the deduction of the emissions and the isotopic composition of atmospheric methane, *J. Geophys. Res., 100*, 11,425-11,446, 1995.

Bzowski, J., J. Kestin, E. A. Mason, and F. J. Uribe, Equilibrium and transport properties of gas mixtures at low density: Eleven polyatomic gases and five noble gases, *J. Phys. Chem. Ref. Data, 19*, 1179-1232, 1990.

Chappellaz, J. A., J. M. Barnola, D. Raynaud, Y. S. Korotkevich, and C. Lorius, Ice-record of atmospheric methane over the past 160,000 years, *Nature, 345*, 127-131, 1990.

Craig, H., C. C. Chou, J. A. Welhan, C. M. Stevens, and A. Engelkemeir, The isotopic composition of methane in polar ice cores, *Science, 242*, 1535-1538, 1988.

Crutzen, P. J., and P. H. Zimmermann, The changing photochemistry in the troposphere, *Tellus, 43*, 136-151, 1991.

Dlugokencky, E. J., P. P. Steele, P. M. Lang, and K. A. Masaire, The growth rate and distribution of atmospheric methane, *J. Geophys. Res., 99*, 17,021-17,043, 1994.

Etheridge, D. M., G. I. Pearman, and P. J. Fraser, Changes in troposheric methane between 1841 and 1978 from high

accumulation-rate Antarctic ice core, *Tellus, 44*, 181-294, 1992.

Etheridge, D. M., L. P. Steele, R. L. Langenfelds, R. J. Francey, J.-M. Barnola, and V. I. Morgan, Natural and anthropogenic changes in atmospheric CO_2 over the last 1000 years from air in Antarctic ice and firn, *J. Geophys. Res., 101*, 4115-4128, 1996.

Etheridge, D. M., L. P. Steele, R. J. Francey, and R. L. Langenfelds, Atmospheric methane between 1000 AD and present: Evidence of antropogenic emissions and climatic variability, *J. Geophys. Res., 103*, 15,979-15,993, 1998.

Fabre, A., J.-M. Barnola, L. Arnaud, and J. Chappellaz, Determination of gas diffusivities in polar firns: Comparison between experimental measurements and inverse modelling, *Geophys. Res. Lett., 27*, 557-560, 2000.

Francey, R. J., M. R. Manning, C. E. Allison, S. A. Coram, D. M. Etheridge, R. L. Langenfelds, D. C. Lowe, and L. P. Steele, A history of $\delta^{13}C$ in atmospheric CH_4 from Cape Grim Air Archive and Antarctic firn air, *J. Geophys. Res., 104*, 23,631-23,643, 1999.

Fung, I., J. John, J. Lerner, E. Matthews, M. Prather, L. P. Stelle, and P. J. Fraser, Three-dimensional model synthesis of the global methane cycle, *Geophys. Res. Lett., 11*, 11,089-11,104, 1991.

Hein, R., P. J. Crutzen, and M. Heimann, An inverse modeling approach to investigate the global atmospheric methane cycle, *Global Biogeochem. Cycles, 11*, 43-76, 1997.

Irion, F. W. et al., Stratospheric observations of CH_3D and HDO from ATMOS infrared solar spectra: Enrichments of deuterium in methane and implications for HD, *Geophys. Res. Lett., 23*, 2381-2384, 1996.

Kandilar, M., and G. J. McRae, Inversion of the global methane cycle using chance constrained programming: methodology and results, *Chemosphere, 30*, 1151-1170, 1995.

Keeling, C. D., and T. P. Whorf, Atmospheric CO_2 records from sites in the SIO air sampling network, in *Trends: A Compendium of Data on Global Change*, Carbon Dioxide Inf. Anal. Cent., Oak Ridge Nat. Lab., U.S. Dep. of Energy, Oak Ridge, Tenn., 2000.

Khalil, M. A. K., and R. A. Rasmussen, Causes of increasing atmospheric methane: depletion of hydroxyl radicals and the rise of emissions, *Atmos. Environ., 19*, 397-407, 1985.

King, S. L., P. D. Quay, and J. M. Landsdown, The $^{13}C/^{12}C$ kinetic isotope effect for soil oxidation of methane at ambient atmospheric concentrations, *J. Geophys. Res., 94*, 18,273-18,277, 1989.

Lassey, K. R., D. C. Lowe, and M. R. Manning, The trend in atmospheric methane $\delta^{13}C$ and implications for isotopic constraints on the global methane budget, *Global Biogeochem. Cycles, 14*, 1-41, 2000.

Lelieveld, J., P. J. Crutzen, and F. J. Dentener, Changing concentration, lifetimes and climate forcing of atmospheric methane, *Tellus, 50*, 128-150, 1998.

Levin, I., P. Bergamaschi, H. Doerr, and D. Trapp, Stable isotopic signature of methane from major sources in Germany, *Chemosphere, 26*, 161-177, 1993.

Levin, I., H. Glatzel-Mattheier, T. Marik, M. Cuntz, M. Schmidt, and D. E. Worthy, Verification of German methane emission inventories and their recent changes based on atmospheric observations, *J. Geophys. Res., 104*, 26,125-26,135, 1999.

Lowe, D. C., C. A. M. Brenninkmeijer, G. W. Brailsford, K. R. Lassey, and A. Gomez, Concentration and ^{13}C records of atmospheric methane in New-Zealand and Antarctica: Evidence for changes in methane sources, *J. Geophys. Res., 99*, 16,913-16,925, 1994.

Lowe, D. C., et al., Shipboard determinations of the distribution of ^{13}C in atmospheric methane in the Pacific, *J. Geophys. Res., 104*, 26,125-26,135, 1999.

Mak, J. E., and C. A. M. Brenninkmeijer, Compressed air sample technology for isotopic analysis of atmospheric carbon monoxide, *J. Atmos. Oceanic Technol., 11*, 425-431, 1994.

Marik, T., Atmospheric $\delta^{13}C$ and δD Measurements to balance the Global Methane Budget, Ph.D. thesis, 120 pp., Univ. of Heidelberg, Heidelberg, Germany, 1998.

Pernaton, E., A. Prinzhofer, and F. Schneider, Reconsideration of methane isotope signature as a criterion for the genesis of natural gas - Influence of migration on isotopic signatures, *Rev. Inst. Francais Petrol., 51*, 635-651, 1996.

Quay, P. D., J. Stutsman, and R. J. Francey, $\delta^{13}C$ of atmospheric CH_4 at Cape Grim, 1991-1995, *Baseline Atmos. Program Australia, 1991*, 110-111, 1996.

Quay, P. D., J. L. Stutsman, D. O. Wilbur, A. K. Snover, E. J. Dlugokencky, and T. A. Brown, The isotopic composition of atmsopheric methane, *Global Biogeochem. Cycles, 13*, 445-461, 1999.

Röckmann, T., Measurement and interpretation of ^{13}C, ^{14}C, ^{17}O and ^{18}O variations in atmospheric carbon monoxide, Ph.D. thesis, 151 pp., Univ. of Heidelberg, Heidelberg, Germany, 1998.

Rommelaere, V., L. Arnaud, and J.-M. Barnola, Reconstructing recent atmospheric trace gas concentrations from polar firn and bubbly ice data by inverse methods, *J. Geophys. Res., 102*, 30,069-30,083, 1997.

Saueressig, G., Bestimmung von Isotopentrennfaktoren in den atmosphärischen Methanabbaureaktionen, Ph.D. thesis, 210 pp., Univ. of Mainz, Mainz, Germany, 1999.

Schwander, J., J. M. Barnola, C. Andrie, M.Leuenberger, A. Ludin, D. Raynaud, and B. Stauffer, The age of the air and the ice at Summit, Greenland, *J. Geophys. Res., 98*, 2831-2838, 1993.

Severinghaus, J. P., and E. J. Brook, Abrupt climate change at the end of the Last Glacial Period inferred from trapped air in polar ice, *Science, 286*, 930-934, 1999.

Snover, A.K., P.D. Quay, and W.M.Hao , The D/H content of methane emitted from biomass burning, *Global Biogeochem. Cycles, 14*, 11-24, 2000.

Stevens, C. M., Atmospheric methane, *Chem. Geol., 71*, 11-21, 1988.

Stevens, C. M., and F. E. Rust, The carbon isotopic composition of atmospheric methane, *J. Geophys. Res., 87*, 4879-4882, 1982.

Tans, P. P., A note on isotopic ratios and the global atmospheric methane budget, *Global Biogeochem. Cycles, 11*, 77-81, 1997.

Thompson, A. M., The oxidizing capacity of the Earth's atmosphere: probable past and future changes, *Science, 256*, 1157-1165, 1992.

Thompson, A. M., and R. J. Cicerone, Atmospheric CH_4, CO and OH from 1860 to 1985, *Nature, 321*, 148-150, 1986.

Trudinger, C. M., I. G. Enting, D. M. Etheridge, R. J. Francey, V. A. Levchenko, L. P. Steele, D. Raynaud, and L. Arnaud, Modeling air mouvement and bubble trapping in firn, *J. Geophys. Res., 102*, 6747-6763, 1997.

Wahlen, M., The global methane cycle, *Annu. Rev. Earth Planet. Sci., 21*, 407-426, 1993.

M. Bräunlich, C.A.M. Brenninkmeijer, P. Jöckel, T. Marik, Air Chemistry Division, Max Planck Institute for Chemistry, P.O. Box 3060, D-55020 Mainz, Germany. (maya@mpch-mainz.mpg.de; carlb@mpch-mainz.mpg.de;

joeckel@mpch-mainz.mpg.de; marik@mpch-mainz.mpg.de)

O. Aballain, J.-M. Barnola, J. Chappellaz, CNRS Laboratoire de Glaciologie et Géophysique de l'Environnement, 54 rue Moliere - Domaine Universitaire, BP 96, 38402 Saint Martin d'Heres Cedex, France. (aballain@glaciog.ujf-grenoble.fr; barnola@glaciog.ujf-grenoble.fr;jerome@glaciog.ujf-grenoble.fr)

R. Mulvaney, Ice and Climate Division, British Antarctic Survey, High Cross Madingley Road, Cambridge CB3 0ET, UK. (R.Mulvaney@bas.ac.uk)

W.T. Sturges, School of Environmental Sciences, University of East Anglia, Norwich NR4 7TJ, UK. (w.sturges@uea.ac.uk)

(Received May 23, 2000; revised February 13, 2001; accepted March 6, 2001.)